Large Scale Radiometric Simulation and Error Assessment of Space Based Objects

Tal Bass[(1)], Patrick North[(2)]

[(1)] Analytical Graphics, Inc. 220 Valley Creek Blvd, Exton, PA, USA Email:tbass@agi.com
[(2)] Analytical Graphics, Inc. 220 Valley Creek Blvd, Exton, PA, USA Email:pnorth@agi.com

ABSTRACT

Predicting the detection, tracking, identification, and characterization performance of various remote sensing systems for near-earth-objects (NEO) and space debris requires modeling and simulation. High fidelity modeling is time consuming and prohibitive when responding to high-priority time-critical events or processing very large quantities of data or parameters. Approximate methods were found to be as much as one thousand times faster than standard evaluation methods, while still agreeing with higher fidelity models as long as certain preconditions were met. We will present both a standard and approximate radiometric space-based object modeling approach to identify the performance and errors associated with each method. We will then recommend the best methods of modeling and simulation based on a number of conditions.

1 INTRODUCTION

One of the greatest challenges to modern space based operations is the growing population of space objects. According to Fig. 1 [1], the number of space objects has been growing steadily for the last half-century and in addition to the tracked space objects the quantity, characteristics, and location of the untracked debris is uncertain. This makes Space Situational Awareness (SSA) a critical piece of space missions, one that relies heavily on remotely sensed observations. However deciding the best tactics and strategies for tasking and collecting these observations, sometimes in response to new data or hypothetical design considerations, is an uncertain art and requires expensive calculations in an ever expanding parametric problem space.

As such, modeling the performance of remote sensing systems is critical for predicting the detection of targets of interest including NEO and space debris. However, because ground-based observations are largely affected by Earth's atmosphere, simulating such systems can require significant computational time to accurately model the propagation of light affected by atmospheric aerosols. The target's material composition, sensor-to-target geometry, and sensor characteristics also affect the detection of these targets. High fidelity, full spectral modeling can therefore be computationally expensive and prohibitive when responding to high-priority time-critical events or processing very large quantities of data or parameters. For this reason, we investigated several modeling approaches of varying fidelity to characterize the performance and error of each. We then developed an approach termed "Fast Metrics" to obtain fast signal calculations as presented here. This approach has been designed to optimize the speed of the calculations while monitoring their fidelity by comparing them to the most rigorous high-fidelity calculations as well as actual measurements collected operationally to assess their accuracy.

2 TEST SETUP

Each modeling approach simulated the detection of 100 satellites from a ground-based remote sensing facility over the span of a year. The orbits of the satellites were randomly generated with altitudes ranging from 6,500 to 49,500 km. The main metrics used to compare the errors associated with each method include Target Intensity, Irradiance at the Entrance Aperture, Signal-To-Noise-Ratio, and Visual Magnitude. The target was treated as a point source such that Signal-To-Noise-Ratio was calculated using Eq. 1.

$$SNR = \frac{S}{\sqrt{S + B}} \tag{1}$$

The signal peak (S) and background (B) were assumed to have a Poisson distribution such that the mean signal is equal to the variance. Here, the background signal B only constitutes the path reflected irradiance of moonlight. Zodiacal light is ignored in all calculations. The sensor exposure time was notionally chosen to be one and ten seconds, such that a separate SNR metric is reported for each value. SNR did not take into account sensor specific values such as the read noise and dark current effects so that the metric is platform agnostic.

The Visual Magnitude was calculated using Eq. 2

$$v = -2.5 \log_{10} \frac{E_{EntranceAperture}}{E_0} \tag{2}$$

where E_0 represents the exoatmospheric irradiance of Vega.

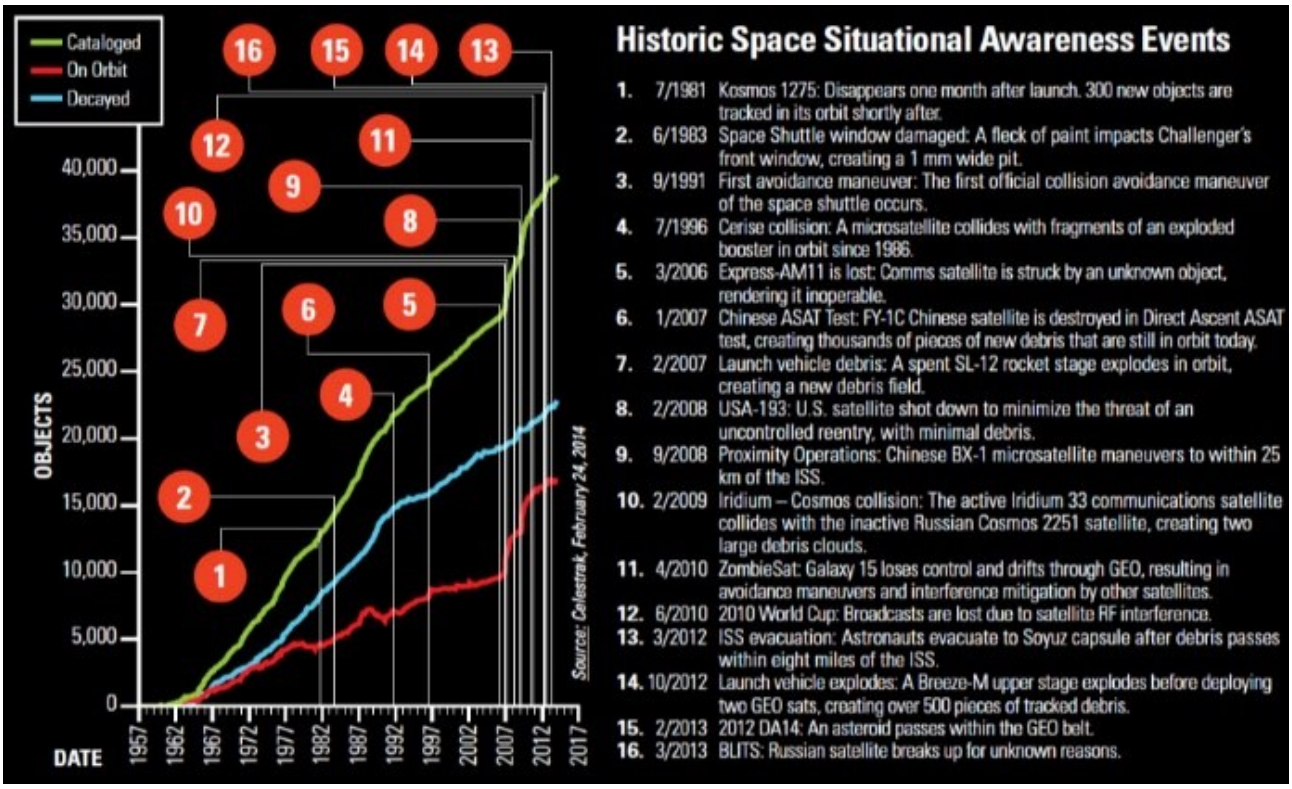

Figure 1. Historic Space Situational Awareness Events [1]

The selected ground-based remote sensing facility is located in Exton, Pennsylvania where AGI owns and operates one of many operational Space Situational Awareness (SSA) sensors collecting on satellites, as shown in Fig. 2. The sensor contained a square vertical and horizontal field-of-view of one-degree and was oriented with a zenith angle of zero. Each satellite shape was approximated to be a one meter sphere of a single, uniform material. Six separate materials were tested in order to compare the effect of various reflectance spectrums on the standard error. The materials tested include Aluminum, Gray Body with 5% reflectance, and Gray Body with 15% reflectance. In addition, a material spectra with 50% reflectance varied by Gaussian noise was modeled, as well as a uniform distribution and a sinusoidal curve with Gaussian noise. The material reflectance spectra (ρ) are shown in Figs. 3-4.

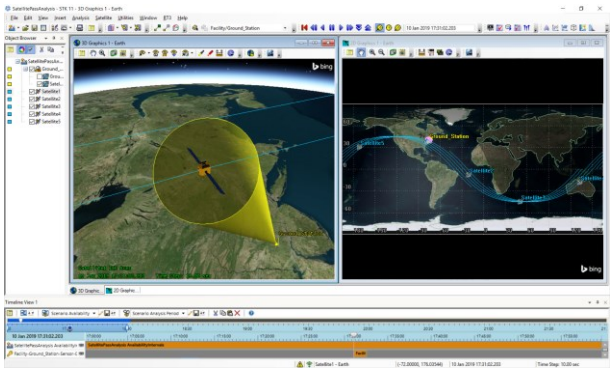

Figure 2. Modeling the SSA sensor Using STK

The reflectance of these materials were used to calculate the target intensity (I_{Target}), calculated using Eq. 3.

$$I_{Target} = \frac{E_{Sun}\, \rho\, Phase(\varphi)\, A_{Target}}{\pi} \qquad (3)$$

where E_{Sun} is the exoatmospheric solar irradiance, φ is the sensor-target-sun phase angle, $Phase()$ is the phase function of the reflection of the target based on the phase angle, and A_{Target} is the cross-sectional area of the target.

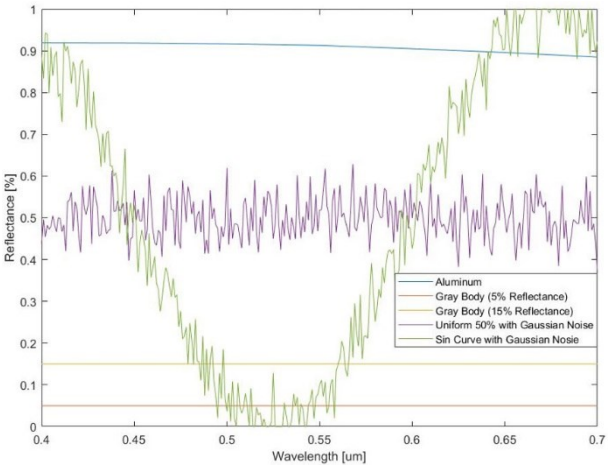

Figure 3. Spectral Reflectance of Sample Materials

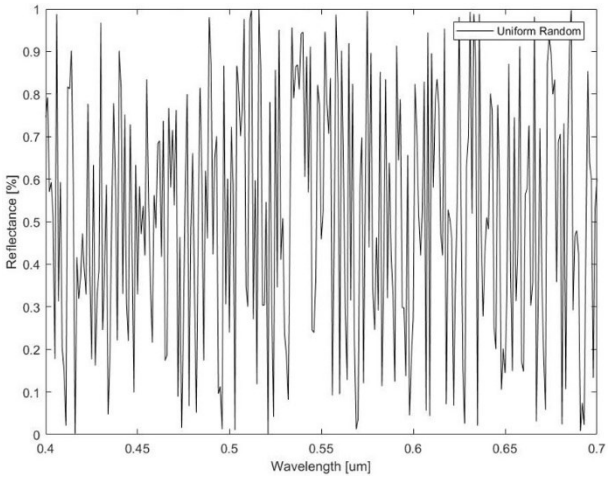

Figure 4. Spectral Reflectance of a Generated Uniform Random Material

Simulations were run using a "Full Spectral Method" which used MODerate resolution atmospheric TRANsmission (MODTRAN) [2], a high-fidelity computer model that calculates optical measurements through the atmosphere, as well as MATLAB [3] code to spectrally integrate.

The Fast Metrics approach was implemented using MATLAB and Systems Tool Kit (STK) [4] written by Analytical Graphics, Inc. STK simulated the satellite orbits and sensor geometry and MATLAB retrieved the geometry from STK to calculate the various metrics. Several approximations were used in this approach in order to generate signal metrics significantly faster than other, higher fidelity models. This Fast Metrics approach used band effective values for all objects while the Full Spectral Method used spectral data sampled at 1 nm for the solar irradiance and material reflectance.

In addition, the Fast Metrics atmospheric transmission (τ_θ) was approximated for targets with zenith angles less than 85 deg using Eqs. 4-5.

$$E_{Target} = \tau_\theta \frac{I_{Target}}{d^2_{TargetToSensor}} \tag{4}$$

$$\tau_\theta = e^{\ln(\tau_{Atmosphere})/\cos\theta} \tag{5}$$

where E_{Target} represents the target irradiance, $d_{TargetToSensor}$ is the distance from the target to the sensor, $\tau_{Atmosphere}$ is the single static atmospheric transmission at zenith, and θ is the target zenith angle from the ground sensor. A graphic of the ground sensor and sample input parameters is displayed in Fig. 5. Here, the angle taken at the target from the sun to the sensor is the phase angle (φ).

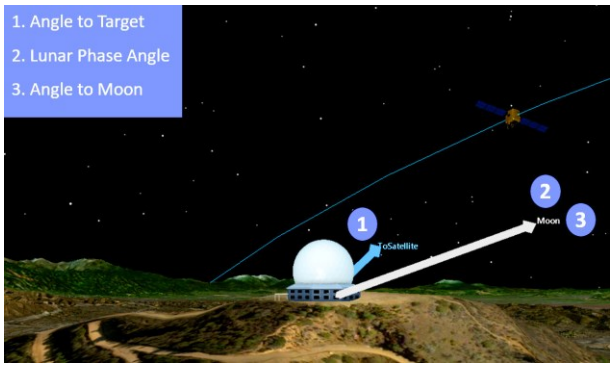

Figure 5. Ground Sensor Graphic Depicting Sample Input Parameters.

Furthermore, the path reflectance from lunar light was approximated to be a constant percentage of the lunar irradiance on the ground at the location of the sensor.

For cases when the lunar zenith angle was greater than 85 deg and less than 99 deg, atmospheric refraction had a significant effect on the path reflectance from lunar light. For such cases the path reflectance was approximated by interpolating the empirical curve shown in Fig. 6.

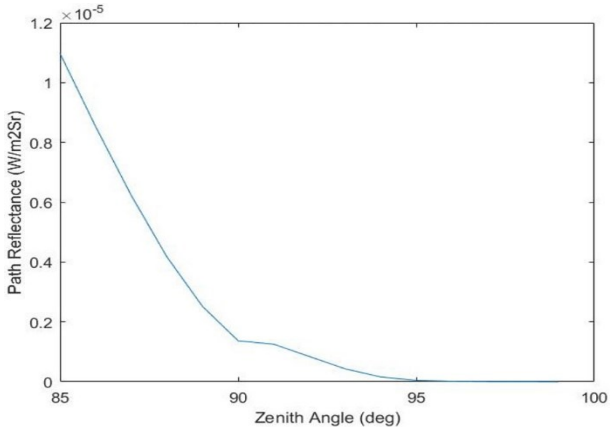

Figure 6. Empirical Curve of the Path Reflectance

MODTRAN was used to generate the empirical curve. The geometry was varied from a lunar zenith angle of 85-105 deg. At each lunar zenith angle, the path radiance was calculated at target zeniths of 15, 30, and 45 deg. These values were than averaged to achieve the curve.

3 RESULTS

Simulating the sensor for one year resulted in the calculation of approximately 2.2 million target signals. Approximately 10% (220,000) of the test points were then calculated using the Full Spectral Method to serve as a basis of comparison.

3.1 Aluminum

The results calculated for an aluminum target are presented in this subsection. Fig. 7 compares the target intensity calculated by the Fast Metrics approach and the Full Spectral Method. Results are shown using aluminum as the material composition for each target.

Results from the two methods agree rather well, as shown in Fig. 7 as expected. The high correlation across results entails that using band effective values to calculate target intensity is a good approximation for aluminum targets across a spread of sensor-to-target geometries.

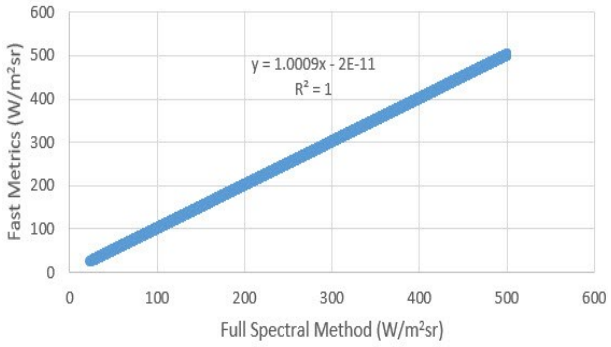

Figure 7. Comparison of Target Intensity for Aluminum

A comparison of the calculated target irradiance values at the sensor is shown in Fig. 8. The atmospheric model used is a significant factor in calculating the target irradiance at the sensor aperture. The high correlation presented in Fig. 8 signifies that the simpler model used to calculate the propagation through the atmosphere in the Fast Metrics calculations (Eq. 4) closely matches the results from the Full Spectral Method in calculating the target irradiance.

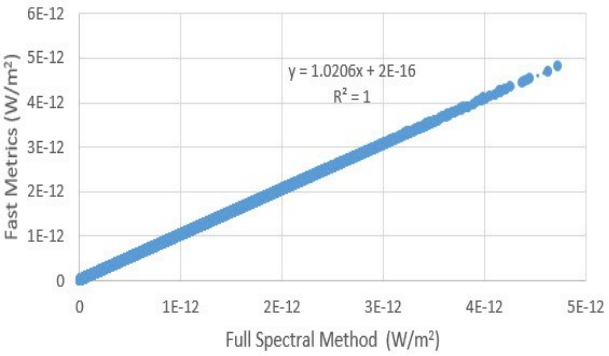

Figure 8. Comparison of Target Irradiance at the Sensor Aperture for Aluminum

A comparison of the total irradiance calculated at the sensor is shown in Fig. 9. The total irradiance is calculated as the sum of the target irradiance and the path radiance from moonlight. Fig. 9 shows a poor correlation between the results calculated using Fast Metrics and the Full Spectral Method. As the target irradiance matches well across methods, the poor correlation is due to the path radiance model used in the Fast Metrics. The Fast Metrics calculations uses a model that approximates the path radiance from moonlight as a constant fraction of the lunar irradiance at the sensor. As a result, this approach does not directly calculate the propagation of the path radiance in order to reduce the computation time. Accordingly, higher fidelity atmospheric models such as MODTRAN should be used when lunar path radiance is an important factor in the signal calculations. In addition, this is a potential area of future work as steps can be made to improve the path radiance model in the Fast Metrics calculations while keeping the computation time to a minimum.

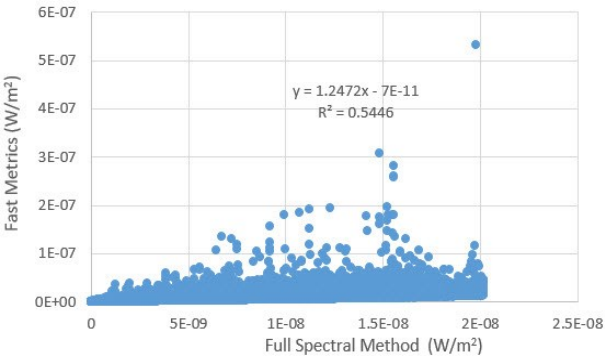

Figure 9. Comparison of Total Irradiance at the Sensor Aperture for Aluminum

The calculated Signal-to-Noise (SNR) ratio using the Fast Metrics calculations and the Full Spectral Method is shown in Fig. 10. The SNR is based on a one second integration time. The results show a very strong correlation, signifying that the Fast Metrics calculations match well with the results from the Full

Spectral Method. An additional trend can be seen in Fig. 10, resulting from the dependency on lunar zenith. When the moon is not visible in the night sky, the path radiance from moonlight is zero and SNR is purely a function of the target irradiance. Since Fast Metrics can accurately calculate the target irradiance, these set of data points have a very high correlation. However when the moon is visible to the ground sensor, SNR is also a function of the path radiance. As the Fast Metrics calculations employ a rather limited model of atmospheric scattering, these data points form a second trend that Fast Metrics do not capture.

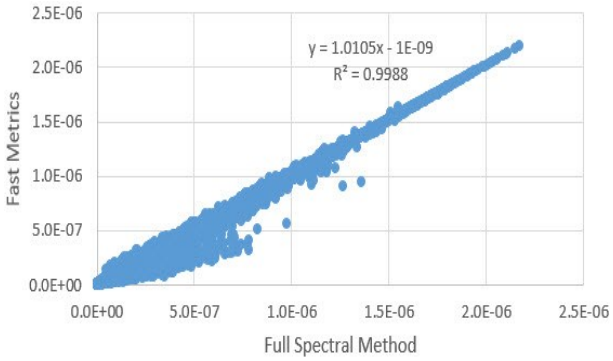

Figure 10. Comparison of SNR for Aluminum Using a One Second Integration Time

Furthermore, Fig. 11 presents SNR for a ten second integration time. The results match quite well with those of Fig. 10, showing that the integration time does not have a noticeable effect on the agreement between methods and we see an improvement of roughly $\sqrt{10}x$.

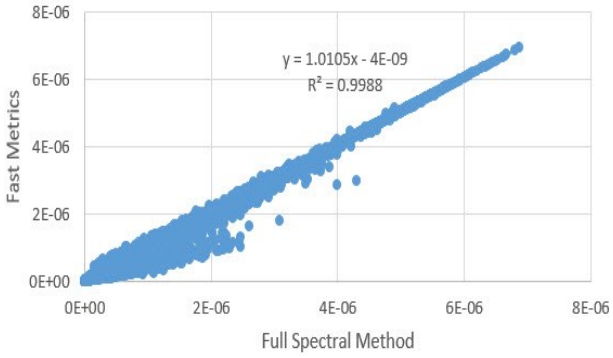

Figure 11. Comparison of SNR for Aluminum Using a Ten Second Integration Time

Finally, Fig. 12 presents a comparison of the calculated visual magnitude. Here visual magnitude is solely a function of the target irradiance, and so the visual magnitude calculated using Fast Metrics correlates rather well with the Full Spectral Method data.

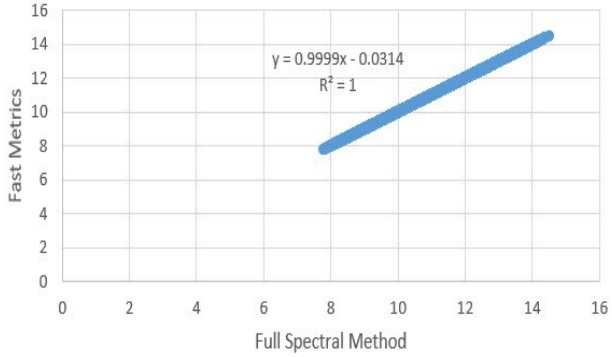

Figure 12. Comparison of Visual Magnitude for Aluminum

3.2 Signal-To-Noise Ratio for All Materials

A comparison of the calculated SNR using Fast Metrics and the Full Spectral Method is presented in this subsection. Figs. 13-24 show the correlation of SNR for each material considered and for both a one second and ten second integration time. Axes titles are omitted after Figs. 13-14 as all of the figures presented in this subsection plot the Fast Metrics values on the y-axis and the Full Spectral Method values on the x-axis.

Figs. 13-24 show that the calculation of SNR using Fast Metrics agrees well across materials. The SNR results for the sinusoidal material (presented in Figs. 21-22) matches noticeably worse than for other materials. This can be attributed to the significant features the sinusoidal material has across the spectrum, such as the reflectance dipping to 0% at 0.52 um and reaching 100% reflectance at 0.65 um. Such features are not captured when using a band effective value for the material. Thus it is not recommended to use Fast Metrics with a single, band effective value for materials that have significant spectral features. Rather, this method should use spectrally downsampled reflectance and atmospheric values with a representative set of spectral samples.

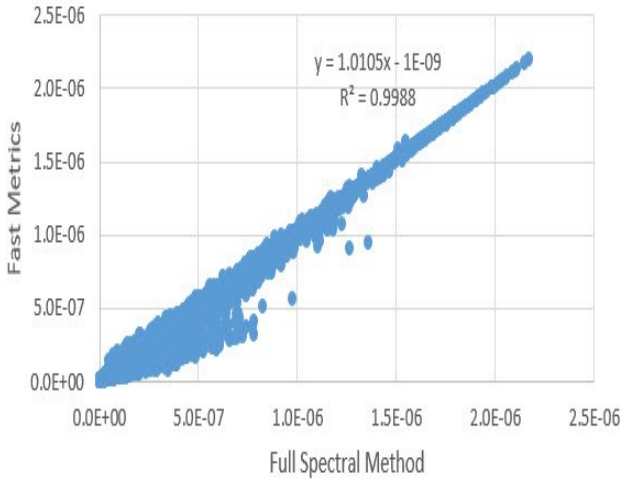

Figure 13. Comparison of SNR for Aluminum Using a One Second Integration Time

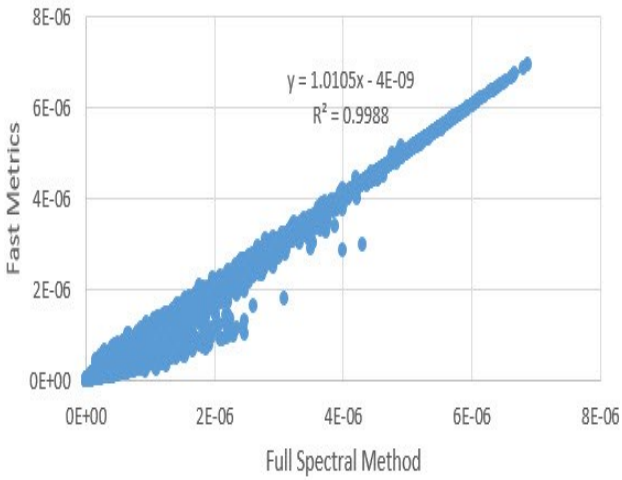

Figure 14. Comparison of SNR for Aluminum Using a Ten Second Integration Time

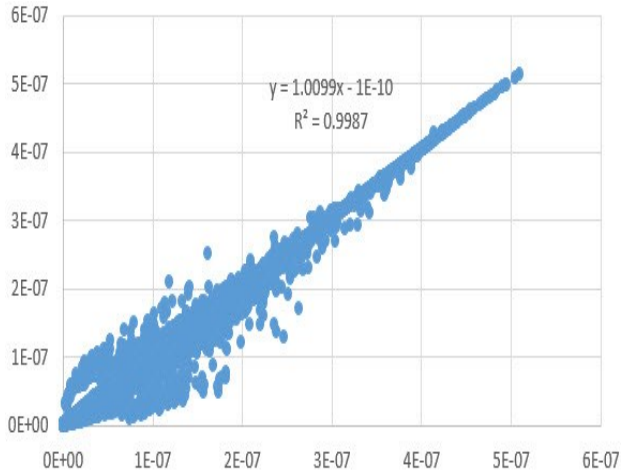

Figure 15. Comparison of SNR for a Gray Body (5% Reflectance) Using a One Second Integration Time

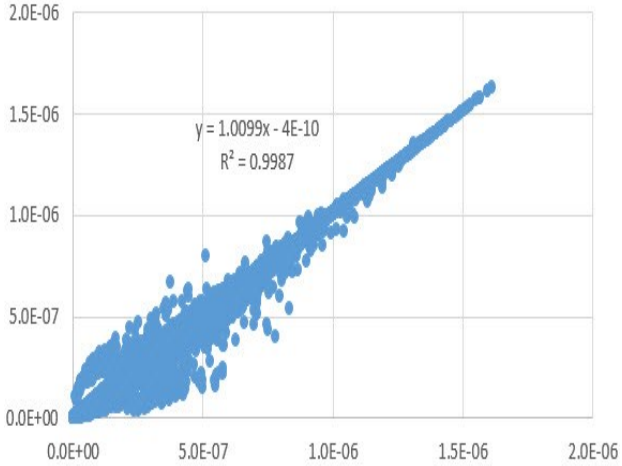

Figure 16. Comparison of SNR for a Gray Body (5% Reflectance) Using a Ten Second Integration Time

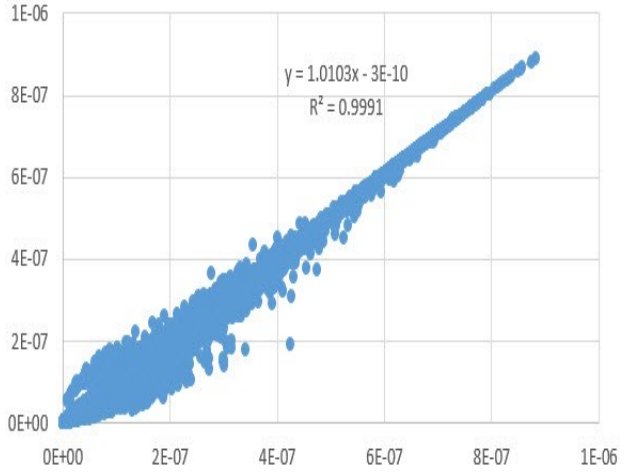

Figure 17. Comparison of SNR for a Gray Body (15% Reflectance) Using a One Second Integration Time

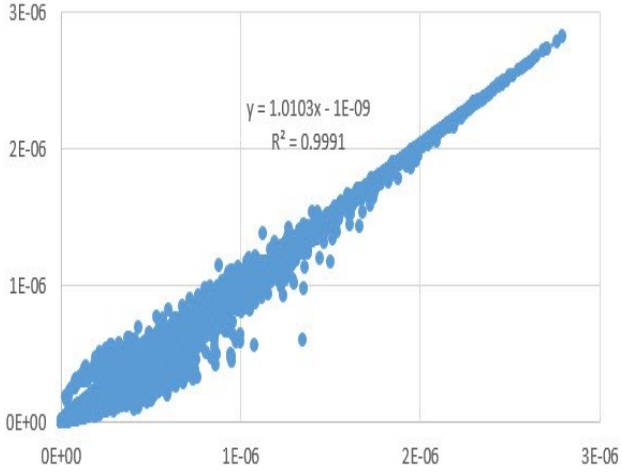

Figure 18. Comparison of SNR for a Gray Body (15% Reflectance) Using a Ten Second Integration Time

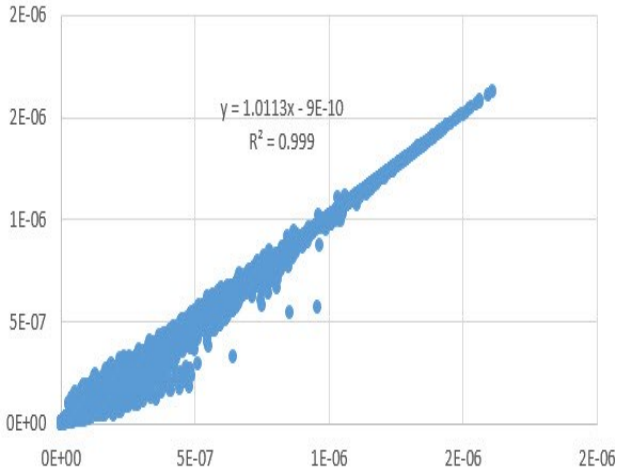

Figure 19. Comparison of SNR for a Material at 50% Reflectance Varied by Gaussian Noise Using a One Second Integration Time

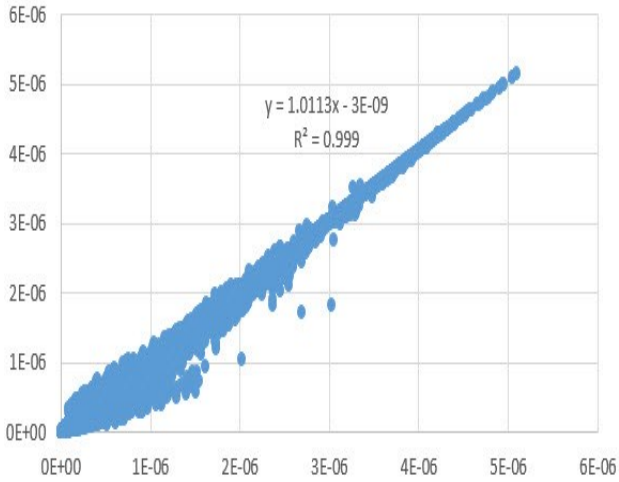

Figure 20. Comparison of SNR for a Material at 50% Reflectance Varied by Gaussian Noise Using a Ten Second Integration Time

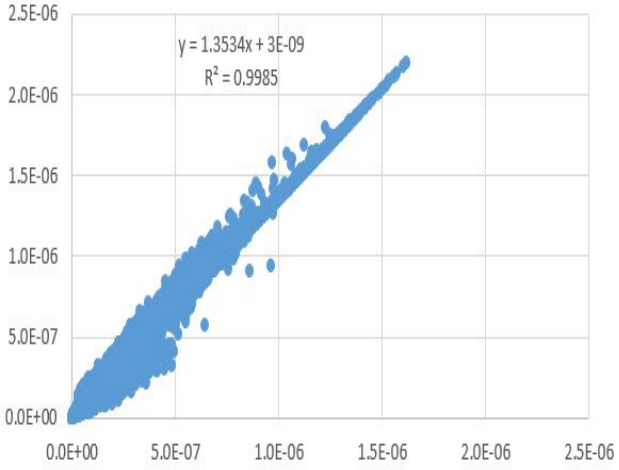

Figure 21. Comparison of SNR for a Material Reflectance of a Sinusoidal Curve Varied by Gaussian Noise Using a One Second Integration Time

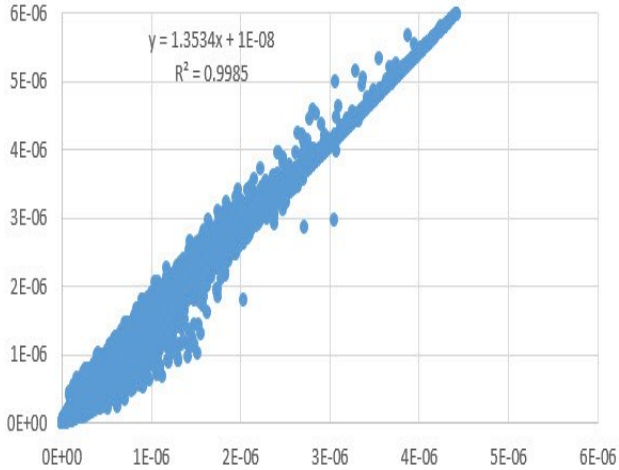

Figure 22. Comparison of SNR for a Material Reflectance of a Sinusoidal Curve Varied by Gaussian Noise Using a Ten Second Integration Time

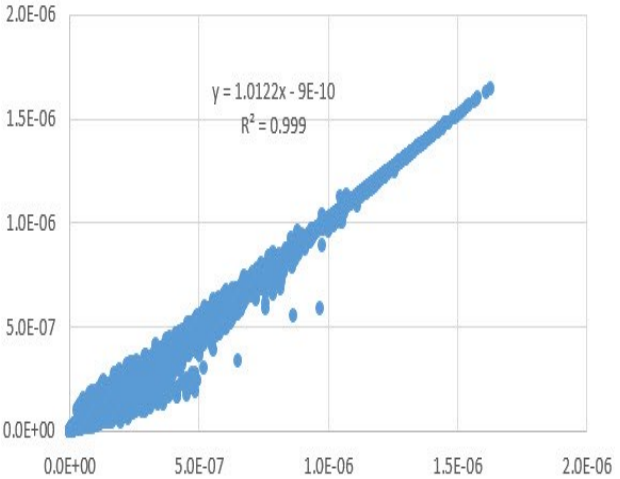

Figure 23. Comparison of SNR for a Uniform Random Material Reflectance Using a One Second Integration Time

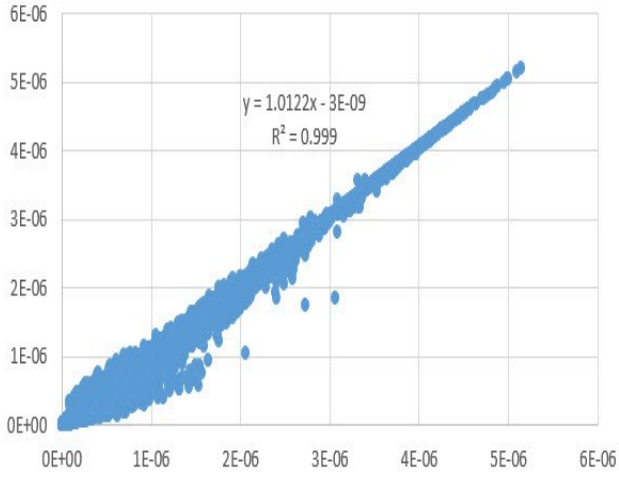

Figure 24. Comparison of SNR for a Uniform Random Material Reflectance Using a Ten Second Integration Time

4 TIMING AND BENCHMARKING

The Fast Metrics calculations were implemented STK Desktop and STK Engine on separate trials to test the performance difference. STK Engine provides an Application Programming Interface (API) to automate capabilities in STK Desktop. As such the results from STK Desktop and STK Engine are identical. However, since STK Engine has less overhead in the case of "No Graphics" mode, STK Engine exhibits faster performance.

Table 1. Computational Time Across Methods

	MODTRAN	Fast Metrics via STK Desktop	Fast Metrics via STK Engine
Calculation Time Steps	220,000	2,205,930	2,205,930
Total Time	04 days 02:00:18	00 days 00:56:17	00 days 00:46:54

Extrapolating the time it took the Full Spectral Method to calculate 220,000 time steps from Tab. 1 out to the total calculation time steps calculated using Fast Metrics, the Full Spectral Method would have taken a total time of 40 days 22 hours and 43 minutes. Thus, the Fast Metrics method is greater than 1,000x faster than the Full Spectral Method. In addition, using STK Engine over STK Desktop provided an increase in speed by roughly 17%. Therefore in cases were graphics are not needed, it is recommended to use Fast Metrics with STK Engine.

As the Fast Metrics results match well with the Full Spectral Method as long as certain caveats hold true, such as using sufficient spectral sampling for target materials that have significant spectral features, it is strongly recommended to use Fast Metrics when applicable. Most notably, in cases where computational time is a critical factor such as large parametric sweeps of signal calculations and other use cases outlined in Tab 2., using Fast Metrics provides a significant advantage without sacrificing fidelity.

4.1 Computer Specifications

Computer specifications of the machine used for all of the calculations are included for benchmarking purposes. The machine used was running Windows 10 and had 16.0 GB installed RAM. In addition the machine had an Intel Core i7 2.70 GHz processor as well as a NVIDIA Quadro M1000M dedicated graphics card.

4.2 MATLAB Optimization

MATLAB's built-in Profile tool was used to optimize the run-time of the Fast Metrics calculations. The Profile tool allows users to track the execution time of functions. One important note about the optimization of the MATLAB scripts is the use of MATLAB's built-in concatenation function called cat. To obtain the data from STK, the Fast Metrics calculations iterate through each satellite in the model and calculates visibility times. The calculations then iterate through each pass of the current satellite and requests geometric parameters such as the range and position of the satellite. After receiving the data for each pass, the Fast Metrics calculations concatenate the data of the current pass to all of the previously stored data using the cat function.

Steps were made to pre-allocate the size of the arrays instead of actively concatenating for each pass. A revised version of the calculations were made that implemented the pre-allocation. Theoretically, this would have sped up the calculations as concatenating data can often be computationally expensive. The revised version of the calculations pre-allocated the memory by creating an array large enough to store data for the theoretical maximum number of visibility times. The data for each satellite would be stored in this array. After storing all of the data, the array would be resized, removing any unused locations. MATLAB's Profile tool was then used to compare the speed of this approach to the speed of the original implementation. Surprisingly, the profiler revealed that it was significantly faster to use MATLAB's cat function then to pre-allocate data. This is most likely due to the relatively slow speed of removing unused locations from the large arrays. In addition, MATLAB's cat function is highly optimized to concatenate arrays quickly such that the time spent concatenating arrays was relatively insignificant to the time spent by the rest of the calculations.

5 ANALYSIS

A heat map of the 220,000 geometric test points used in the analysis is provided in Fig. 25 to show the parametric diversity of the simulations. The lunar phase angles are plotted against the lunar zenith angles for each test point. The spread of the data shows each geometric condition was sampled sufficiently to be statistically relevant.

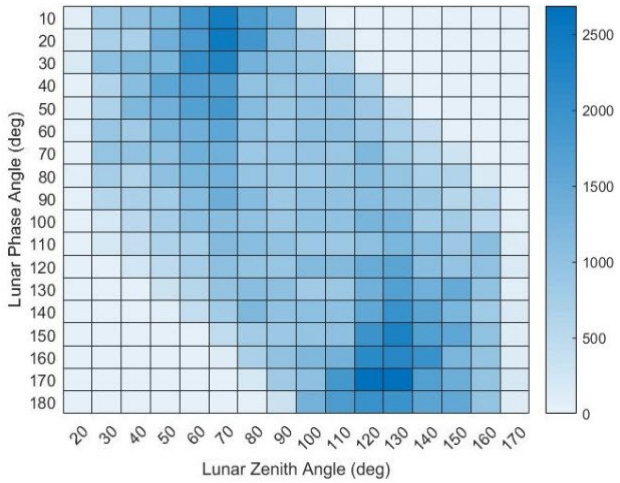

Figure 25. Heat Map of the Test Point Geometries

Fig. 26 presents the spectral irradiance for a test point calculated by the Full Spectral Method. Here, aluminium is used as the target material. Fig. 26 shows the solar irradiance at the satellite, the reflected satellite irradiance at the Earth prior to any atmospheric model, and the satellite irradiance at the sensor after the atmospheric model is applied. Absorption features can be seen in the solar irradiance at 431 and 517 nm from Iron, 486 and 657 nm from Hydrogen, and 589 nm from Helium and Sodium. In addition, an atmospheric absorption feature can be seen at 687 nm from Oxygen. This feature causes a significant dip in the final target irradiance but not in the solar irradiance due to the significant presence of Oxygen in the atmosphere.

Because the Full Spectral Method uses a small sampling width of 1 nm, these spectral features are explicitly captured in the target irradiance and directly affect the sensor's final SNR as calculated by the Full Spectral Method. However since the Fast Metrics calculations use Band Effective values, the results calculated by Fast Metrics only indirectly take such spectral features into account. Furthermore, the effect of Rayleigh scattering can be seen in the large dip in target irradiance values from 400-450 nm. Such effects are not captured in the Fast Metrics calculations due to the simpler, band-effective atmospheric model used. Thus it is not recommended to use single band Fast Metrics with materials that have significantly different reflectance values for blue light than light at other parts of the spectrum.

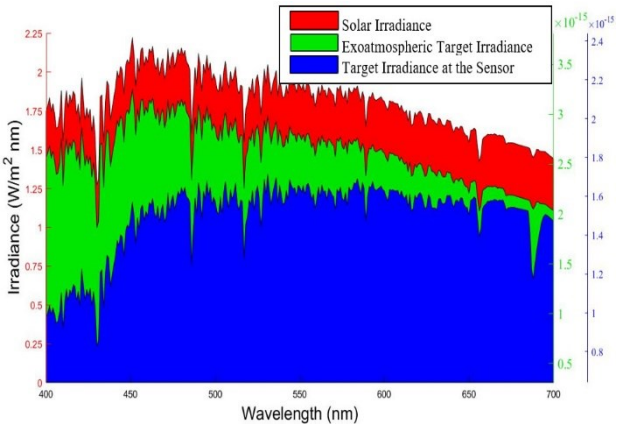

Figure 26. Propagation of Spectral Irradiance Using MODTRAN

6 USE CASES

There are a number of scenarios where calculating the signal of objects in space is important. SSA is especially important to satellite owners and operators, and is primarily a function of detecting and characterizing the observations of both satellites as well as scanning the adjacent areas for potential objects including space debris and Near-Earth-Objects (NEO). AGI developed the Commercial Space Operations Center (ComSpOC) [5] to collect SSA data commercially for satellite owners and operators and their mission operations team shared a number of real-world scenarios where fast signal calculations would be useful. Tab. 2 shows specific examples of common tasks at various mission phases.

Table 2. A Sample Set of Mission Phases and Tasks Requiring Signal Calculations

Mission Phase	Tasks Requiring Signal Calculations
New Missions and Research	Design, Test, and Characterize Performance for: • New Sensor Systems • Detection Algorithms • Collection Modes of Operation • Targets of Interest
Initialization and Operations	• Schedule Planning • Detecting Odd Orbits • Difficult Solar, Celestial, or Galactic Backgrounds • Site Selection and Performance Prediction
Time Critical Situations	• Anomalies • Loss of Contact • Loss of Attitude Control • Bad TLE Data • No Show Problems

One such example was satellite Shijian-17 (SJ-17) when from Nov - Dec 2018 the observed visual magnitude did

not match predictions at different points of the collection windows. Using the Fast Metrics calculations, 400 sample observations from operational collection conditions were generated in 18 seconds and compared to the empirical measurement over a period of one month from an observation site in Dubbo, Australia as shown in Fig. 27. Using Fast Metrics with the default satellite model values, there is already excellent agreement with a visual magnitude difference from empirical measurements of less than 5%, as shown in Tab. 3. Because the Fast Metrics calculations include various simplifications (such as modelling the satellite as a uniform, aluminium sphere), certain trends are not captured. This plus inherent noise in measured data results in a lower correlation in the data as shown in Fig. 27. However despite these assumptions, there is still good agreement between the Fast Metrics calculations and the measured values. Accordingly, results show that with many assumptions very fast calculations can be utilized in time critical situations or for very large data analysis.

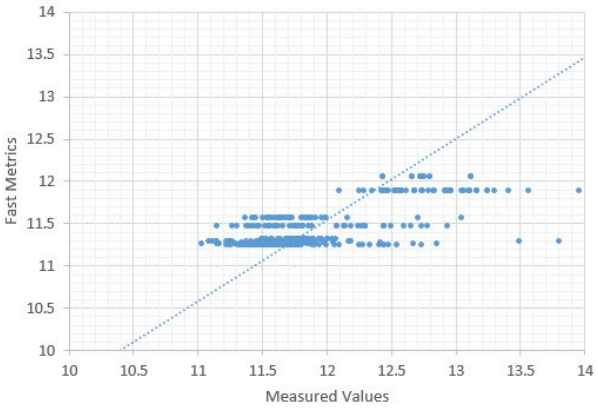

Figure 27. Comparison of Visual Magnitude for SJ-17

Table 3. Visual Magnitude Accuracy of Fast Metrics Calculations for SJ-17

Average Percent Error	3.72%
Standard Deviation	2.82%

7 CONCLUSION

Fast calculations for predicting the detection, identification, and characterization performance of remote sensing systems were found to be as much as one thousand times faster than standard evaluation methods. These fast calculations largely agreed with higher fidelity models and operationally measured empirical data. In certain use cases, such as time critical events and analysis containing a very large amount of data, fast calculations can be used when higher fidelity modeling is prohibitive.

The Fast Metrics calculations contain many assumptions that must be handled carefully. It is recommended to use sufficient spectral sampling for target materials that contain significant spectral features. As the calculations implement a simple atmospheric approximation, it is also not recommended to use the current Fast Metrics lunar path radiance model when this is an important factor.

Because of the significant increase in speed, implementing Fast Metrics calculations can improve the efficiency of various SSA operations. As the amount of space objects orbiting Earth and the number of observational sensors measuring such objects continue to increase, Fast Metrics will provide a scalable solution for modeling the performance of remote sensing systems while agreeing favourably with higher fidelity models.

8 REFERENCES

1. Kelso, T.S. (2000). Celestrak. Online at *http://www.celestrak.com* (as of 11 January 2019).
2. Berk et al. (2005). MODTRAN (TM) 5, a reformulated atmospheric band model with auxiliary species and practical multiple scattering options: Update. In *Proc. Algorithms and Technologies for Multispectral, Hyperspectral, and Ultraspectral Imagery XI,* SPIE. 5806. 662-667. 10.1117/12.564634.
3. The MathWorks, Inc. MATLAB Primer R2017a. Online at *https://www.mathworks.com/help/releases/R2017a/pdf_doc/matlab/getstart.pdf* (as of 3 January 2019).
4. Analytical Graphics, Inc. Engineering Tools. Online at *http://agi.com/products/engineering-tools* (As of 2 Jan 2019).
5. Hall, R. & Johnson, T. (2016). Commercial SSA Catalog Performance. *In Proc. 17th. ISCS 'Advanced Maui Optical and Space Surveillance Technologies Conference'*, AMOS, Maui Economic Development Board, Inc.